15ÈMES JOURNÉES DE L'HYDRODYNAMIQUE
22 - 24 novembre 2016 - Brest

Conception et étalonnage d'un hydrophone à base de PVDF étiré à 25 μm d'épaisseur

Handmade 25 μm thin PVDF based hydrophone and its calibration

Pavel Mostovykh, **Michel Arrigoni**
ENSTA Bretagne, Institut de Recherche Dupuy de Lôme, FRE CNRS 3744, 2 rue François Verny, 29806 Brest Cedex 09

Résumé

Ce travail présente les étapes vers la fabrication d'un capteur de pression universel possédant une large dynamique de mesure comprise entre une fraction de kPa jusqu'à des dizaines de GPa en amplitude et avec une large bande passante allant de quelques fractions de Hz jusqu'à quelques centaines de MHz en fréquence. L'élément principal est une jauge de contrainte de type "Bauer shock gauge" élaborée à partir de difluorure de polyvinylidène (PVDF) disponible sur le marché. Un assemblage comportant cette jauge est utilisé comme un hydrophone flottant. De part sa minceur, cet hydrophone demeure peu intrusif dans l'eau et résiste aux chocs. Il est montré que cet hydrophone est linéaire en amplitude et possède une sensibilité en fréquence modérément variable. Il offre une précision comparable à celle des hydrophones classiques dans leur domaine d'application. Comme inconvénient, le dispositif proposé dépend fortement de l'orientation et ne peut donc être utilisé que dans des expériences où la direction du son ou la propagation de l'onde de choc est bien prévisible à l'avance.

Summary

A step towards manufacturing a universal pressure sensor, capable to operate between fraction of kPa and tens of GPa in amplitude, between fractions of Hz to hundreds MHz in frequency is described. As a primary element, a market–available polyvinylidene difluoride Bauer shock gauge is used. A simple device based on this gauge is calibrated as a floating hydrophone. This hydrophone is minimally intrusive in the water stream, and is shock–resistant. It is shown that such a hydrophone is linear in amplitude and has a moderately variable frequency sensitivity. It provides comparable to conventional hydrophones accuracy in their range of applicability. As a drawback, the proposed device is strongly orientation–dependent, and therefore can be used only in experiments when the direction of the sound or the shock wave propagation is well predictable in advance.

1 Introduction

This paper originated from our strong belief that a pressure gauge capable to measure pressure variations in liquids and solids at the same time, and electrically adjustable to measure pressures between fractions of kPa to several GPa can be proposed. Evidently, this gauge will be, in most cases, less accurate than the specifically designated instrumentation for a particular task. However, such gauge is important if the task of measuring significantly different types of signals in the same setup is imposed (for example, measuring underwater acoustics and underwater shock wave propagation with the same instrument).

2 Development

2.1 Considerations sustaining the choice of PVDF

As a primary sensitive element we chose the so–called Bauer shock gauges (Lee, Graham, Bauer & Reed 1988), which are primarily used for measuring impact pressures on the solid body surfaces. These gauges are made of polyvinylidene fluoride, or polyvinylidene difluoride (PVDF, also known as PVF_2). Its chemical formula is $(-CH_2 - CF_2-)_n$. This polymer has several modifications, one of which is a strong ferroelectric polymer.

This choice is based on the great variety of applications that PVDF has been reported to have. Apart from the already mentioned Lee et al (1988), who used it up to hundreds of kbar with response times of the order of ten nanoseconds, Shuheng & Wenfan (2015) reported a PVDF based infrasound sensor capable to work in the 3–30 Hz range, and to measure signals from general infrasound generators for the corresponding range. Wang & Toda (1999) have studied PVDF in the intermediate frequency range — they've implemented it for a sound generator, and received two resonance frequencies at 31 kHz and 59 kHz. However, no information of using PVDF in this enormously wide frequency band as the same mechanical entity has been thus far reported. This is our final goal.

This paper reports our first data obtained in water, i.e. data concerning PVDF gauge as a hydrophone. To facilitate using of the same gauge in different environments, we decided to avoid using any type of backing material, letting the gauge float in water. This approach has both some promising advantages and some evident disadvantages. We would name here the following:

- the water–PVDF acoustic impedance mismatch is relatively small (about 2.5 times), and so the reflected waves from the gauge are significantly weakened;
- in addition, the gauge thickness is below 1 mm, so the back–and–forth in it is below 1 μs; as a result, the secondary reflected wave from the gauge back surface nearly merges with the primary reflected wave from the front surface, and annihilates it;
- therefore, the proposed gauge is minimally intrusive in the flow;
- however, the gauge is no longer firmly positioned in water, and its location, including its orientation, cannot be specified exactly;
- the gauge, under some circumstances, can be subjected to resonance oscillations in its width or in its length from the point where it is attached to the rigid support;
- the gauge averages the pressure acting on its surface; for instance, if the active area has the shape of a square with the side 5 mm, it will have the first interferometry minimum at the wave frequency 300 kHz, and close and higher frequencies will be significantly damped by the gauge;
- moreover, the gauge can move during the measurements due to the water stream.

The last point is the most important one. On one hand, it seems to be an apparent disadvantage — for example, if we measure the duration of the shock positive phase, due

to the gauge motion with the after–shock water stream it will register a longer phase than it really is (luckily, this effect has the order of the ratio of the liquid particles velocity to the wave velocity, that is generally not very high, and at least conventional hydrophones do not operate under transonic conditions). On the other hand, a light gauge entrained into water is less sensitive to the current than a fixed gauge is. In linear acoustics, since the relation between acoustic pressure and acoustic–induced speed is known, and this relation is linear, the hydrodynamic effects are by itself included in the hydrophone calibration coefficient (more exactly, since these effects are frequency– and orientation–dependent, they are included in the frequency sensitivity curve and the directivity curve). However, under hydrodynamic shock loading, the hydrodynamic effects would not scale proportionally to the shock overpressure, conventional hydrophone sensitivity to hydrodynamic impact becomes a source of hardly predictable error. Therefore, the last point can be viewed as an advantage also, at least for some types of experiments.

2.2 Underwater experimental set–up and equipment

PVDF hydrophone calibration was fulfilled in a water pool of ENSTA Bretagne. Its dimensions are 3 m wide, 4 m long and 2.75 m deep, and the water in the tank is tap water kept at the temperature of 12–18°C. The sketch of the experimental set–up is presented in figure 1. It consisted of an ultra–sound generator with nominal generation frequency of 100 kHz, and two hydrophones: a calibrated one, RESON TC4034-1[1], and our handmade device. The latter was manufactured as follows:

- the 25 mm^2 Bauer shock gauge was used as a primary element. The biggest active area available, made of gold deposited electrodes (square 5 mm×5 mm), was chosen since we intend to measure low (for this technology) pressure signals. This gauge is a stripe of 25 mm×60 mm×25 μm (fig.2);
- the leads were extended with copper conductive tape, and the opposite ends of the tape were fixed in an AMPHENOL FFC/FPC card connector;
- this connector was welded to the inner cables of two identical RG174, 6 m long coaxial cables ending with BNC plugs. The outer conductors of the two coaxial cables were connected between each other;
- the gauge was covered with 50 μm thick PVDF adhesive insulator from both sides;
- the resulted structure was electrically shielded and hydroproofed with a 80 μm thick adhesive aluminium tape that was rolled around the gauge's end, and was left in contact with itself 10 mm on each side of the gauge;
- the described construction, together with the leads, was attached to one end of a long screw; the other end of the screw remained above the water, and was used to adjust the depth and the orientation of the gauge in the water.

As a result, the thickness of the gauge reached the value 0.59–0.63 mm, width 50 mm, and the active area was located 10 mm apart from the bottom edge; the total length of the gauge (without the screw) exceeded 100 mm. The screw was long enough to get its opposite end out of the water level in our experiments. The photos of the parent element and the PVDF hydrophone with the graph paper used as a background are shown in figure 2.

It was not possible to measure the angular position of the gauge accurately; the techniques used visually located the straight bottom edge of the gauge relative to the square mesh on the bottom of the water tank. This method is assumed to give ±5° accuracy, so that it is appropriate to estimate the orientation–induced effects in the measurements, but not to quantify them exactly.

[1] http://www.teledyne-reson.com/download/hydrophone_data_sheets__/TC4034.pdf

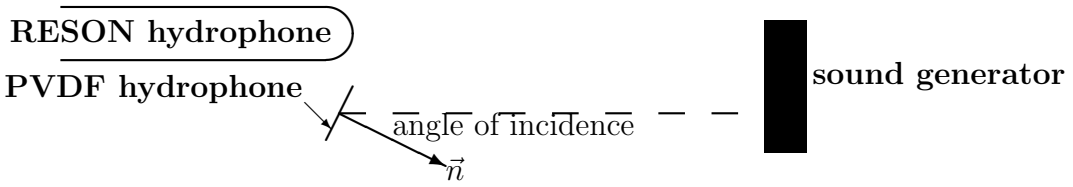

Figure 1: Sketch of the experimental set–up for hydrophone calibration (view from above).

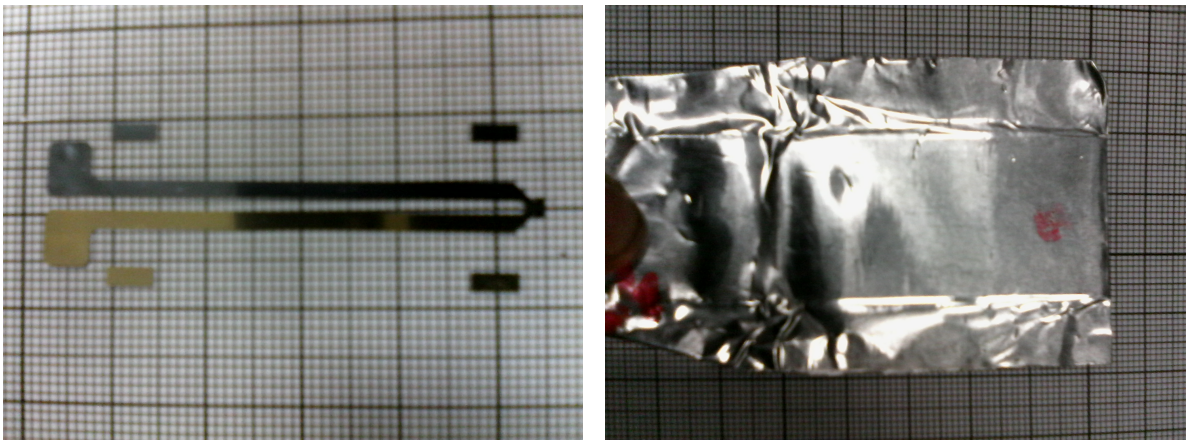

Figure 2: The Bauer shock gauge — the parent element used in the production of hydrophone (left, active area 1 mm^2) and the resulting device (right). The right spot shows the active area location.

From the electrical point of view, the RESON hydrophone was via Voltage preamplifier RESON VP1000 connected to the National Instruments (NI) 10–channel acquisition card, whereas the two leads of our handmade hydrophone were connected via Kistler charge amplifier models 5011 and 5018, respectively, to the same card. The passbands of the amplifiers were 1 MHz.

The measurements were performed at two distances between the emitter and the hydrophones (the distance between the hydrophones was negligible) — 500 mm and 1000 mm. The three elements were submerged 780 mm from the water surface, and more than 1 m of water was left from the three other sides, and also behind the hydrophones, so that no waves except the direct one could be measured within the first 1 ms. An example of the pressure–time histories acquired by the NI card is shown in figure 3. The four graphs show the Kistler charge amplifier 5018, Kistler charge amplifier 5011, the calibrated RESON hydrophone and the water in the water tank, respectively. The part of the signal between 0 (the time instant of the start of generation) and 0.2 ms corresponds to the parasites, and we can see that our handmade hydrophone (or its cables) receive several times more noise than the water in the pool, whereas the RESON hydrophone and its cable are securely protected. However, during the reception phase, time between 0.35 and 0.6 ms, the "water" signal shows that there are no longer any parasites, and the measured signal corresponds to the water pressure. What is also important, at this highest generation voltage of 398 V both hydrophones show symmetric signal (the importance of this observation becomes clear if we consult the real pressure values as seen by the RESON hydrophone as a function of its supply voltage presented in figure 4. The most negative pressure value is well below 0, and the non–cavitating shape of the pressure–time history was not mandatory to occur).

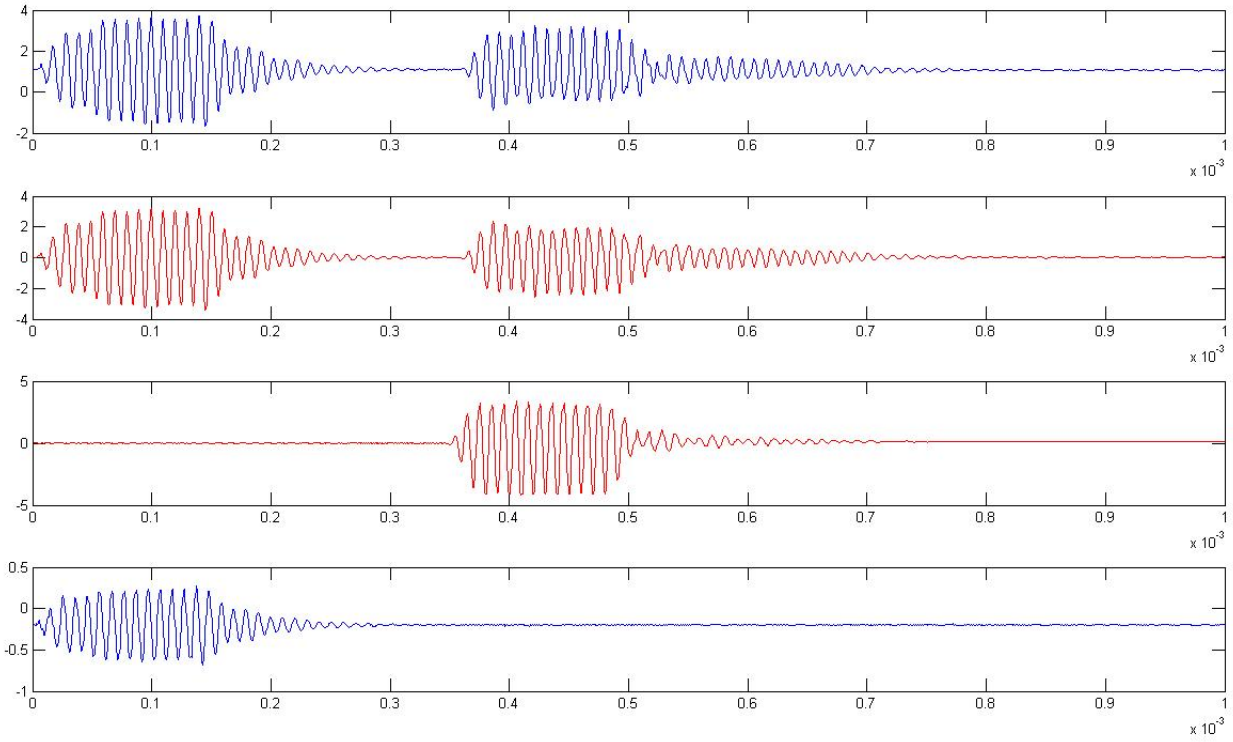

Figure 3: The last, hundredth, shot at zero angle of incidence, from a distance of 500 mm at 398 V, 100 kHz of generator supplier. Top: our PVDF hydrophone lead connected via Kistler charge amplifier # 5018; next: another lead of our PVDF hydrophone connected via Kistler charge amplifier # 5011; third: calibrated RESON hydrophone with RESON VP1000 Voltage preamplifier; last: electrical parasites in the water tank.

Apart from distance and depth, the experimental conditions are specified by:

- the angle between the positive normal to the PVDF hydrophone and the direction from the hydrophone towards the emitter (we distinguish the "front" and the "back" surfaces of our hydrophone by putting a mark on the front one);
- the emitter supplying voltage (not more than 400 V);
- the emitter supplying frequency;
- the duration of the sound emission;
- the settings of the three amplifiers.

The calibration experiment, including both initiating the sound emission and recording, is computer–controlled, and is repeated 100 times with each particular settings for error estimation.

The data processing included the following steps:

- constant offset was subtracted from each channel;
- the 100 repetitions were averaged for each channel at each time instant, and the corresponding standard deviations obtained;
- the Hilbert transform was calculated for each of the averaged signals, and then the modulus of the complex amplitude was evaluated;
- based on the distance between the generator and the hydrophones, the speed of sound in water and the duration of the sound emission, the interval between 30% and 95% of the wave train passing through the measurement point was determined;
- the average pressure voltage amplitude in the wave and the standard deviation of the measurement are taken as the average and standard deviation of the amplitude modulus in the aforementioned interval, respectively;

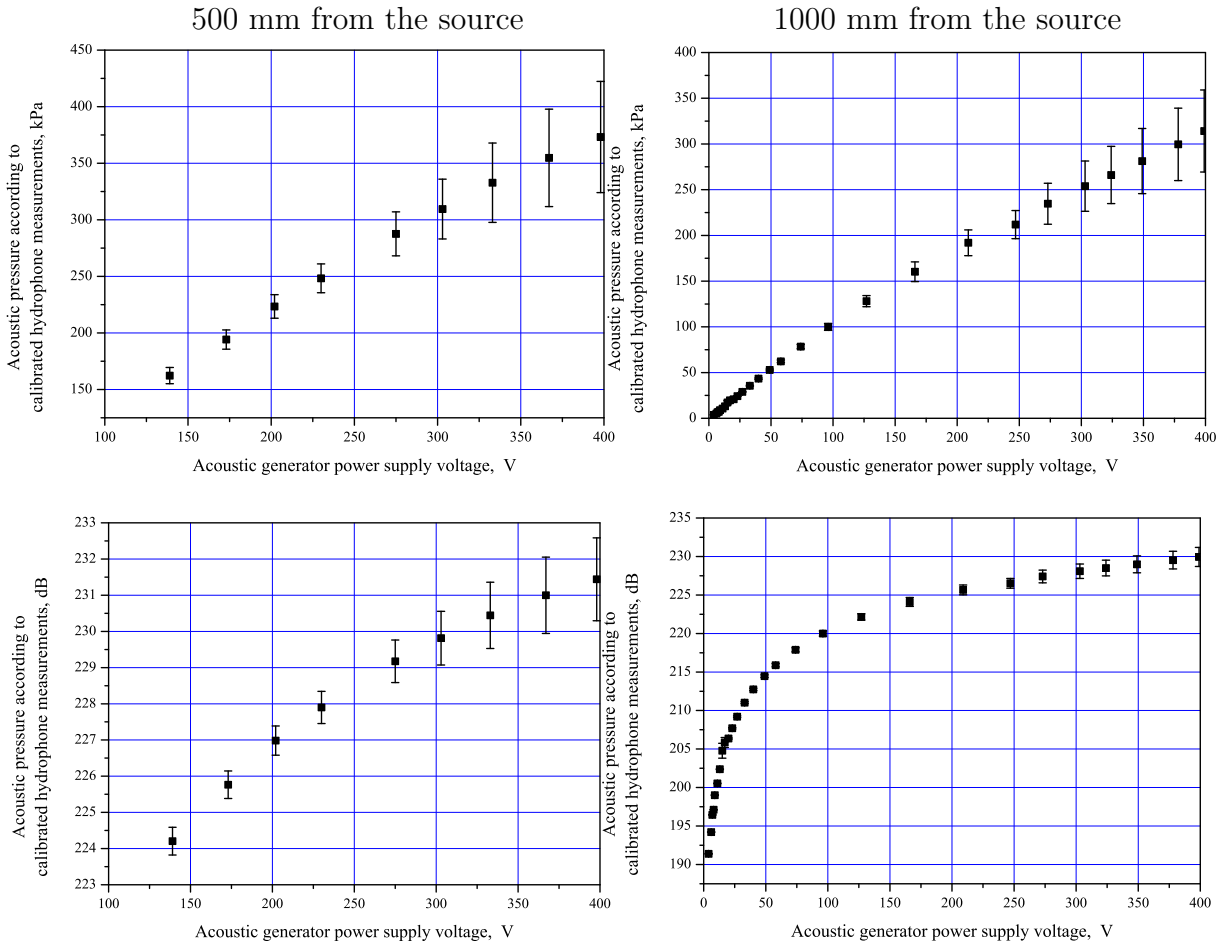

Figure 4: PVDF sensitivity coefficient vs generator supply voltage. Dimensional kPa (top row), logarithmic dB re 1V/μPa (bottom row). Distance between the generator and the hydrophones 500 mm (left), 1000 mm (right).

- pressure amplitude is recalculated using the frequency–dependent RESON hydrophone sensitivity curve;
- sensitivity of our handmade hydrophone, independently for both leads, was therefore determined as a function of amplitude, frequency and orientation.

Coincidence of the supposed and the actual pressure wave frequencies was checked manually, and some experiments were withdrawn (for instance, 35 kHz of emitter supplying voltage resulted in a harmonic, 105 kHz sound wave, being much stronger the "main" one).

Also, manually the standard deviation resulting from the Hilbert–transform–based amplitude variation in time was compared with the shot–to–shot variation for each channel. Physically, the former standard deviation (SD) is primarily to the non–sinusoidal shape of the sound wave, that results in some ambiguity in the amplitude viewed by the Hilbert transform method. The latter SD includes several phenomena, such as non–reproducibility of the emission (in amplitude, but also in time after the computer trigging), floating PVDF hydrophone displacement, etc. For most experiments done, the former SD exceeded the latter. This effect was especially pronounced at high voltage supplied to the emitter (when non–sinusoidal shape is, indeed, more likely to occur), and for the fixed RESON hydrophone (since timing was more repeatable). Conversely, at the smallest voltages tested, and for the floating PVDF hydrophone, the latter SD exceeded the former 2–3 times. However, the SD plotted on the graphs includes only the former, and not the latter part, in all cases.

Table 1: Amplification settings used for the KISTLER charge amplifier model 5011, model 5018, and the RESON Voltage preamplifier as a function of the generator power supply for the series of experiments shown on figure 5, right. All the rest experiments were done with the settings specified in the top line.

Voltage range V	No. of tests	KISTLER 5011 pC/V	KISTLER 5018 pC/V	RESON dB
270...400	6	30.8	30.80	+0
70...269	6	15.4	15.40	+6
30...69	4	7.70	7.70	+12
20...29	3	3.08	3.080	+20
9...19	5	1.54	1.540	+26
4...8	4	1.54	0.770	+32

2.3 Experimental results

2.3.1 Sound field generated

Figure 4 shows the pressure levels generated by the emitter on its nominal frequency 100 kHz at 500 mm and 1000 mm along the normal to it. Both increasing and decreasing of the emitting frequency resulted in significant decrease of the sound pressure. We can suppose from these data that in the vicinity of the emitter a cavitation cloud should have been present during the experiment; we have an independent reason to claim that since the bubble collapse induced noise was easily heard. However, this cloud caused just slightly noticeable change in the nearly linear dependence of acoustic pressure vs voltage supplied to the emitter (figure 4, left top). In addition, this cloud increased the acoustic pressure SD at high driving voltage.

2.3.2 Amplitude dependence of handmade PVDF–based hydrophone

Amplitude dependence was measured at the nominal frequency of 100 kHz, and the results are presented in figure 5 showing the dependency of the calibration coefficient (in fC/Pa or pC/kPa) with respect to the acoustic pressure. The SD of the PVDF sensitivity at different pressure intensities are relatively high, whereas acoustic pressure amplitude was varied nearly two orders of magnitude. We confirm that PVDF is linear and hysteresis–free in the considered domain, as assumed elsewhere (Hyndman & Gaffney 1989). The two leads of PVDF, which are referred respectively to PVDF1 and PVDF2, gave signals 1.2 times different, but it is most likely due to the difference in the electronic circuits used in the two different charge amplifiers and their acquisition lines (the settings used are given in table 1). This claim is justified by the change in hydrophone sensitivity following the change in the settings, especially at low generation voltage, where higher amplification was used.

What has no explanation at all, is the strong (about 2 times) difference in the calibration coefficients at the two different distances.

2.3.3 Frequency dependence of handmade PVDF–based hydrophone

Frequency dependence was studied for normal (180°) and 135 degrees incidences, and shown in figure 6. Though the frequency range tested is relatively narrow, the results show evident, non–monotonic change in the hydrophone sensitivity. Even though we do not see any periodic structure in the frequency sensitivity curves obtained, we think that

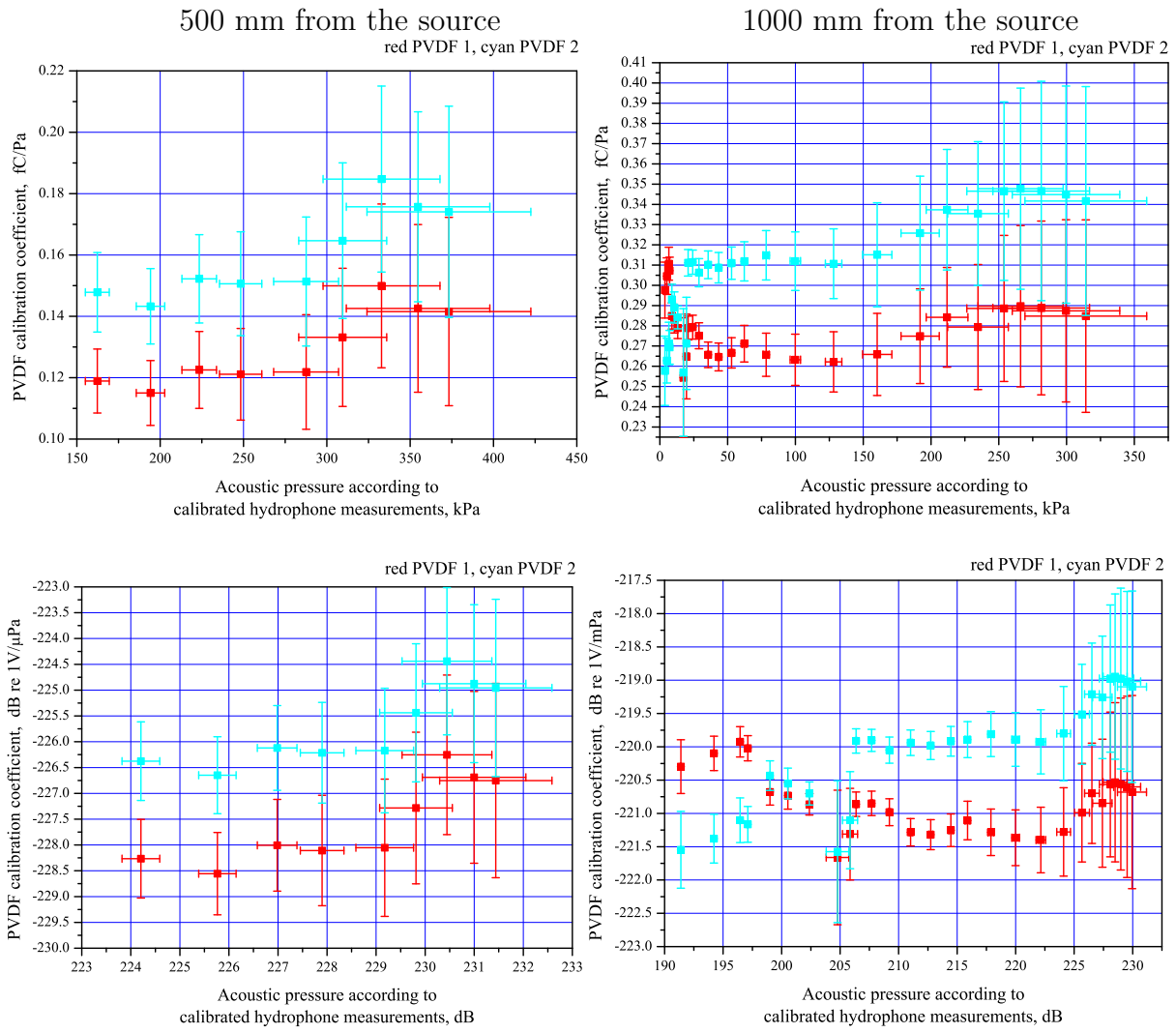

Figure 5: PVDF sensitivity coefficient vs acoustic pressure amplitude measured by the calibrated RESON hydrophone. Dimensional fC/Pa vs kPa (top row), logarithmic dB re 1V/μPa vs dB re 1 μPa (bottom row). Distance between the generator and the hydrophones 500 mm (left), 1000 mm (right).

the explanation for these curves lies in the wave–gauge interaction patterns, related to the gauge geometrical sizes, and not in the PVDF material characteristics itself.

The top row compares two different distances between the generator and the hydrophones, under the same angle. The difference in the sound wave amplitude for the two cases is included in the sensitivity coefficient calculation, and so the only significant difference between the two sets of data is that the hydrophones were installed independently for the two series of experiments (in each series, the equipment was **not** moved intentionally between the shots at different frequencies. It could, theoretically, have moved due to the water currents, though no such displacement was noticed by the end of each series). Based on figure 6, top, we can state the following:

- the frequency dependence is repeatable in the two series;
- the actual sensitivity value is, on average, 25% lower for the 500 mm distance case. As proposed above, our explanation of this fact is the sensitivity angular dependence due to the $\pm 5^\circ$ positioning inaccuracy; this question is further discussed in § 2.3.4.

The shape of the curve on the bottom figures differ: maximum sensitivity occurs at a higher frequency around 110 kHz, compared to 90 kHz for the normal incidence case.

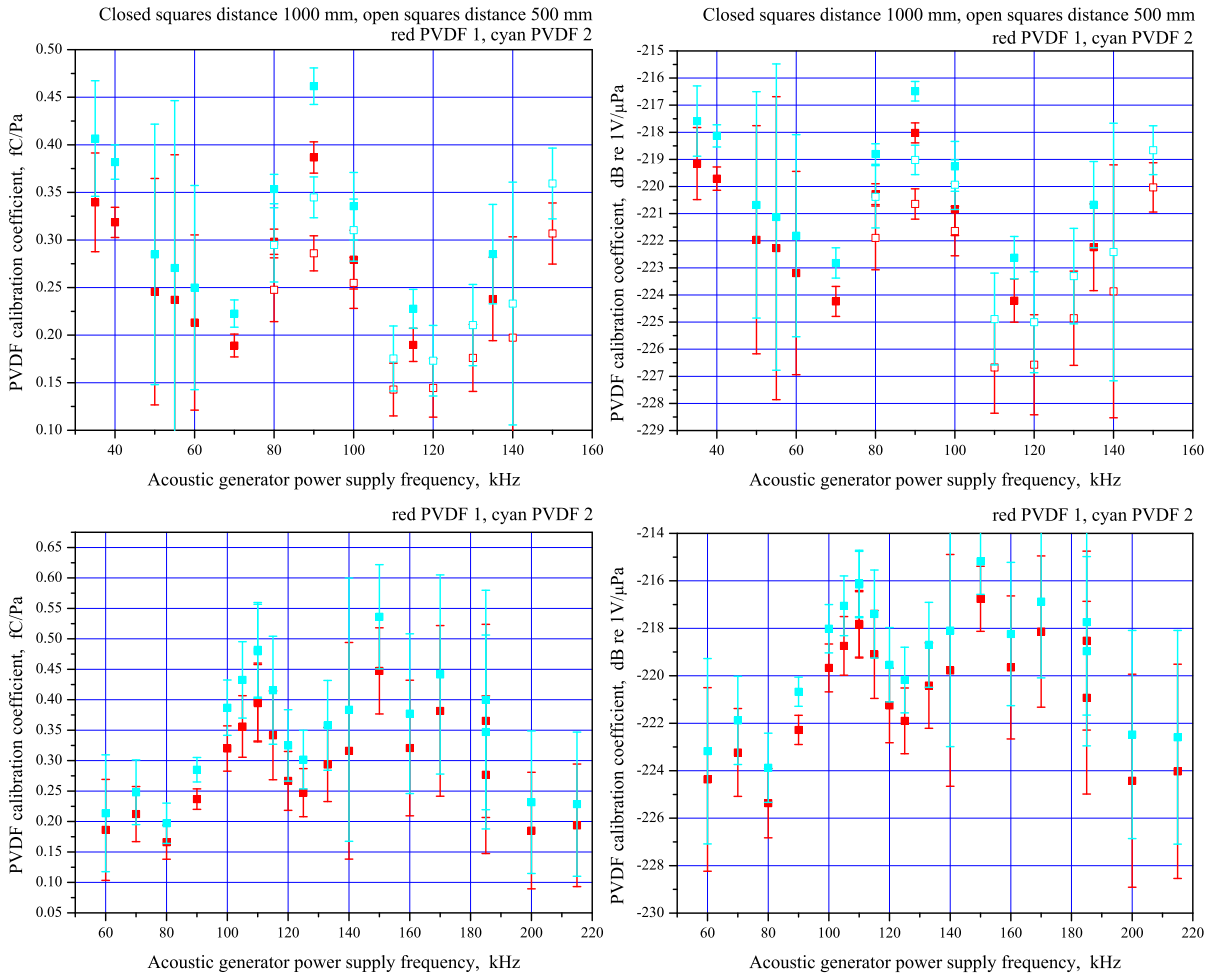

Figure 6: PVDF sensitivity coefficient vs generator supply frequency. Dimensional fC/Pa (left column), logarithmic dB re 1V/μPa (right column). Angle of incidence of the handmade PVDF hydrophone 180° (top), 135° (bottom). In the top row, the distance between the generator and the hydrophones 1000 mm (closed square points), 500 mm (open square points); in the bottom row, only the distance 500 mm presented.

2.3.4 Angular dependence of handmade PVDF–based hydrophone

Figure 7 shows experiments conducted at the emitter nominal frequency with both supply power voltage and hydrophone incidence angles varied. The figure on the left shows some increase in the RESON hydrophone signals in the 135° incidence case. We attribute this increase to partial wave reflection from the PVDF plane towards the RESON hydrophone; the sketch of their relative position is presented in figure 8. The semi–improvised "nozzle" that is formed between the oblique PVDF plane and the RESON hydrophone head parallel to the sound wave, causes local pressure increase on the side of the RESON hydrophone.

However, the effect evidenced on the PVDF hydrophone, is so much stronger than the one on RESON, that additional explanations are necessary. The lowest sensitivity at normal incidence excludes the speculations on the influence of the active area size relative the sound wavelength, since in the normal incidence case the wave front is parallel to the active area. If we suppose that a PVDF plate impacted obliquely is less free to move than in case it is impacted normally, we would obtain a qualitative explanation of the sensitivity variation observed; however, the difference between absolutely free and absolutely fixed wall in terms of pressure load is only two times, whereas the effect on figure 7, right, is between two and three times. We suppose that this difference is related to 3D loading of the PVDF material in the oblique case.

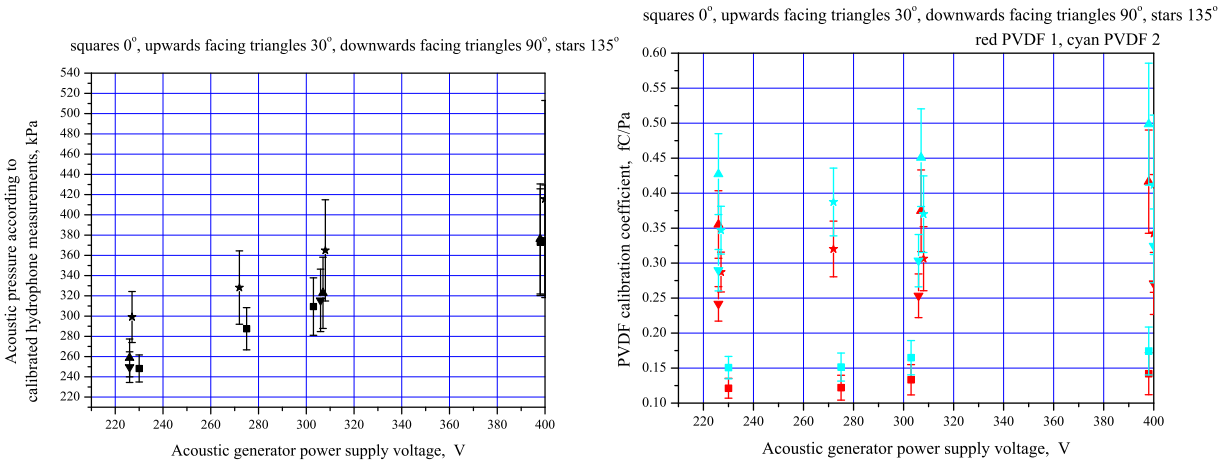

Figure 7: RESON (left) and PVDF (right) hydrophone amplitudes at different generator power supply voltages (abscissae) and at different geometrical orientations of the PVDF gauge (types of points).

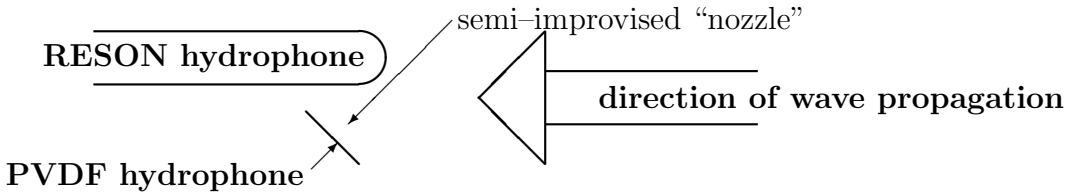

Figure 8: Sketch of the mutual hydrophone location in the 135° incidence case (top view).

2.4 Comparison with the theoretical models of PVDF

Strictly speaking, in order to predict theoretically the piezoelectric behaviour of PVDF gauges, we need to study the wave propagation in them coupled with the wave propagation in the surrounding water, that makes the problem fairly complicated. We may, however, first study two cases, which we can, in some sense, consider as limiting:

- hydrostatic compression of PVDF. It would have been the case of a small gauge (compared to the sound wavelength);
- 1D strain compression of PVDF. It would have been an approximation to a very big gauge case, when no in–plane deformation in PVDF is induced. It is only an approximation, since it assumes existence of in–plane stresses in PVDF, that will vary on the length of the acoustic wavelength, but it can still be viewed as an opposite limiting case.

If we denote 1, 2 the in–plane directions, 3 the out–of–plane direction, the mechanical boundary conditions will take the form $\sigma_1 = \sigma_2 = \sigma_3 = -p$ and $\varepsilon_1 = \varepsilon_2 = 0$, $\sigma_3 = -p$, respectively. Numerical values of the hydrophone sensitivity in the ideal charge amplifier circuit for several piezoelectric properties matrices proposed for PVDF in the literature (Schewe 1982; Childs 2000; Marty 2002; Liu, Pan, Lin & Lai 2013; Bauer & Varadan et al 1989), are summarized in table 2.

Comparison of these values with the measured hydrophone sensitivities is presented in figure 9. The models appear to be divided into two groups:

- Schewe (1982), Childs (2000) and F. Bauer & Varadan et al (1989)[2] fairly well describe the behaviour at normal incidences, and underestimates the PVDF sensitivity

[2]This last model is composed of F. Bauer data for piezoelectric coefficients, reported in a private communication, and Varadan data for mechanical coefficients

Table 2: PVDF material sensitivity under hydrostatic compression and 1D out–of–plane strain compression, according to several references. All numbers in fC/Pa.

ref	hydrostatic compression	1D out–of–plane strain compression
Schewe (1982)	0.0750	0.271
Childs (2000)	0.0675	0.209
Marty (2002)	-0.952	0.883
Liu, Pan, Lin & Lai (2013)	0.575	0.718
F. Bauer & Varadan et al (1989)	0.0850	0.132

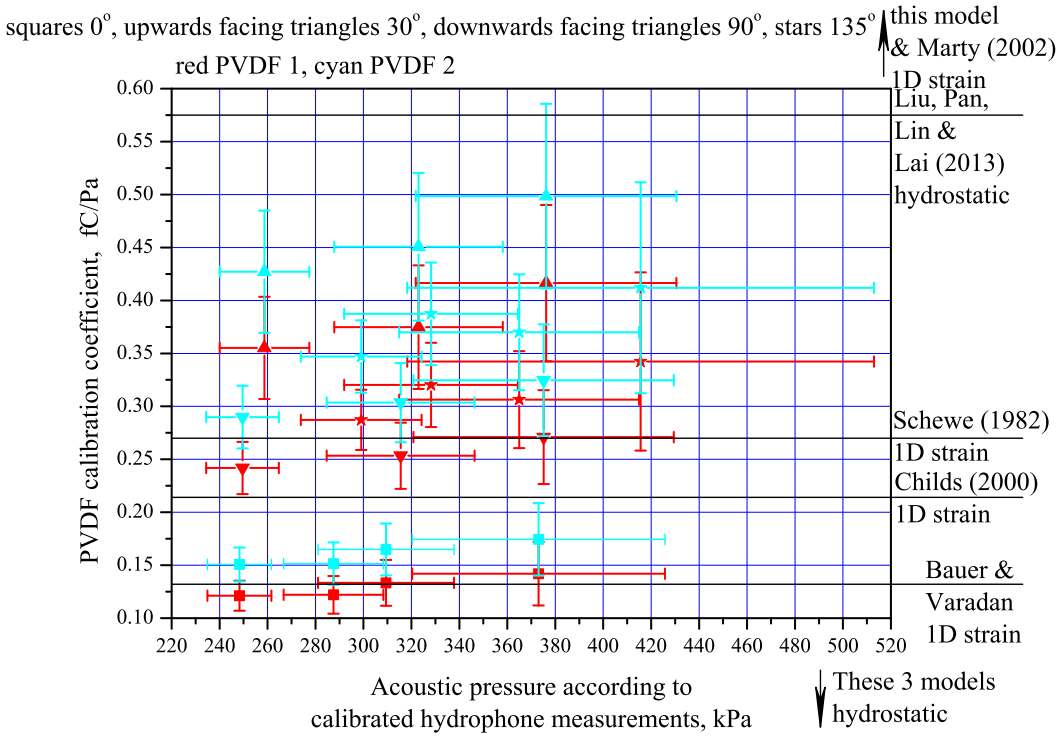

Figure 9: Comparison of the handmade PVDF hydrophone sensitivity at different angles of incidence and different pressure levels (data of figure 7) with the theoretical values predicted in the literature (Schewe 1982; Childs 2000; Marty 2002; Liu, Pan, Lin & Lai 2013; Bauer & Varadan et al 1989).

to oblique waves;

- Marty (2002) and Liu, Pan, Lin & Lai (2013) slightly overpredict the 30° sensitivity, and strongly overpredict all other orientations[3].

[3]It worth making one remark at this point. All coefficients in table 2 are positive, except the one for hydrostatic compression in the model of Marty (2002). According to the numbers in this publication, the lateral effects in PVDF are so important that they change the **sign** of the generated charge. If it were true, all the values achieved in the present experimental campaign are valid, and, in addition, polarization of the charge generation should have been established. This was not done, partly because the existence of this question was not known then, partly because mutual localisation of the two hydrophones was not perfect enough to tell the phase shift between their signals

3 Conclusion

A calibration of a floating hydrophone, using PVDF Bauer shock gauge as the sensitive element, is fulfilled. It is shown that such a hydrophone is strongly orientation–dependent, and therefore can be used only in experiments when the direction of the sound or the shock wave propagation is well predictable in advance. A characterisation of the frequency dependence of this PVDF based hydrophone is obtained between 40 kHz and 200 kHz. It is also pointed out that the charge given by the PVDF leads is dependent of the acquisition line. For a given orientation, the distance does not affect the frequency response, but it affects in our case the calibration factor.

We are fulfilling experiments with weak shock waves in order to evidence the difference between fixed and floating hydrophones behaviours under acoustic loading, on one hand, and shock loading, on the other hand.

Acknowledgements: Authors want to thank Region Bretagne for its financial support through the Stratégie Attractivité Durable program. Authors are also greatly indebted to Michel Legris and Irène Maupin from ENSTA Bretagne for their precious support on the use of hydrophone and acquisition system.

References

H. Schewe Piezoelectricity of Uniaxialiy Oriented Polyvinylidene Fluoride, IEEE Ultrasonics Symposium Proceedings, 1982, pp. 519–524.

L. Lee, R. Graham, F. Bauer, R. Reed. Standardized Bauer PVDF piezoelectric polymer shock gauge. Journal de Physique Colloques, 1988, 49 (C3), Suppl. 9, pp. C3-651-C3-657.

V. V. Varadan, Y. R. Roh, V. K. Varadan and R. H. Tancrell Measurement of All The Elastic and Dielectric Constants of Poled PVDF Films Ultrasonics Symposium, pp. 727–730, 1989.

D. A. Hyndman, E. S. Gaffney Calibration of PVDF transducers at stresses below 1 MPa. The Sixth American Physical Society Topical Conference on Shock Compression of Condensed Matter. 1989. Eds S. C. Schmidt, James N. Johnson; L. W. Davison. ISBN 044488271/9780444882714. Pp. 809–811.

Hong Wang, and Minoru Toda Curved PVDF Airborne Transducer IEEE Transactions on ultrasonics, ferroelectrics, and frequency control, vol. 46, no. 6, 1375–1386, november 1999.

Ashley Erin Childs Modeling and analysis of thin-film, piezoelectric actuators A thesis submitted in partial fulfillment of the requirements for the degree of Master of Science in Mechanical Engineering, Montana State University, Bozeman, Montana, January 2000.

Pierre Noël Marty Modelling of Ultrasonic Guided Wave Field Generated by Piezoelectric Transducers. PhD Thesis, University of London, March 2002.

Z.H. Liu, C.T. Pan, L.W. Lin, H.W. Lai Piezoelectric properties of PVDF/MWCNT nanofiber using near-field electrospinning Sensors and Actuators A, vol. 193, pp. 13–24 (2013).

Shi Shuheng, Wang Wenfan Development of a High Precision Infrasonic Sound Sensor International Journal of Signal Processing, Image Processing and Pattern Recognition Vol. 8, No. 9 (2015), pp. 211–218.